P. P. Sorokin*
J. R. Lankard*
E. C. Hammond†
V. L. Moruzzi

Laser-pumped Stimulated Emission from Organic Dyes: Experimental Studies and Analytical Comparisons

Abstract: Stimulated emission spectra of two organic dyes, chloro-aluminum phthalocyanine (CAP) and 3,3'-diethylthiatricarbocyanine iodide (DTTC) are compared. Giant-pulse ruby laser excitation was used in both cases. An end pumping configuration employed with DTTC resulted in narrow beam divergences and high conversion efficiencies. For CAP, the oscillating transition is one which terminates on an excited vibrational level of the ground electronic state. For DTTC, stimulated emission at the lowest concentrations occurs at the peak of the Franck-Condon-shifted fluorescence band but moves to longer wavelengths as the concentration is increased. The transient behavior of the CAP laser, pumped in a transverse geometry, was observed and compared with computer solutions of the rate equations. Polarization measurements of the laser beams were also made. An analysis is given of requirements for achieving optimal pumping by means of flashlamps.‡ [The paper concludes with an addendum reporting recent observations of stimulated emission from dye solutions lasing at wavelengths ranging from blue (4385 Å) to orange (6000 Å)].

1. Introduction

In separate communications[1,2] we recently reported observations of ruby-laser-pumped stimulated emission from two organic dyes, chloro-aluminum phthalocyanine (hereafter, "CAP"), and 3,3'-diethylthiatricarbocyanine iodide (hereafter, "DTTC iodide"). CAP, the dye with which the effect was discovered, emits a coherent beam of light in a fairly broad band of frequencies (~40Å wide) centered (in ethyl alcohol solvent) at $\lambda = 0.756\mu$. DTTC iodide, the dye studied subsequently, radiates a beam comprising an even broader band of frequencies (100-200Å wide), centered in the spectral region 0.80-0.86μ, the exact position depending upon the solvent used (Sec. 2), and, more importantly, upon the dye concentration (Sec. 4).

In both cases, we initially employed a single technique in which the beam from a giant-pulse ruby laser was made to impinge transversely upon a cell filled with a specific dye solution and located within a secondary cavity (Fig. 1). Subsequently, for the DTTC iodide we employed an end-pumping configuration (Fig. 2), one result being that this more symmetrical method of pumping[2] afforded much lower output beam divergences. (A half-angle divergence as small as ~0.5 milliradian has been observed with the secondary cavity mirrors (mirrors M_1 and M_2) separated by 22 cm; still less divergence should, in principle, be attainable through the use of mirror apertures that alter diffraction loss. Illustrating the flexibility of cavity design that is possible in this connection, it was found that the end-pumped dye laser continued to work quite well when the spacing between mirrors M_1 and M_2 was increased to 1 meter, the dye cell being repositioned to remain roughly equidistant between the two mirrors.) The solvent first used in the CAP laser experiment was ethyl alcohol; the first observations of stimulated emission in DTTC iodide were obtained using either ethyl alcohol or methyl alcohol.

In the present paper we set out to give a rather complete summary of the data we have so far gathered for these new laser systems. First, effects of solvent variation will be taken up in Sec. 2; then, in Sec. 3, we give an energy level interpretation of the lasing action as it occurs in the case of each dye. In Sec. 4 we discuss the shift in the spectral position of the DTTC iodide stimulated emission band produced by a change in the dye concentration. Next, in Sec. 5, we examine conversion efficiencies measured with the end-pumping configuration and, in Sec. 6, give results of measurements of the CAP laser pulse shape along with some comparisons of those results with computer solutions of the rate equations. In Sec. 7, we remark on the symmetry of the combining states and on the nature

* Work partially supported by Army Research Office, Durham, N. C. under Contract DA-31-124-ARO-D-205
† Morgan State College, Baltimore, Maryland
‡ Successful efforts toward this end are reported in the separate communication on page 148.

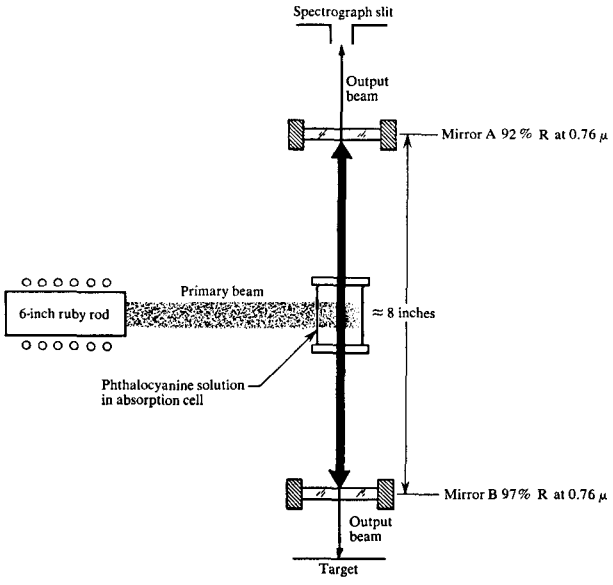

Figure 1 Transverse pumping arrangement employed initially for both dyes. It is shown here with mirrors appropriate for the CAP laser. Various other mirror reflectivities and spacings were employed.

of the spectral transitions connecting them, and speak of the polarization properties of the laser beam as we have deduced and measured them. Finally, in Sec. 8, we advance some considerations toward the possibility of pumping organic dye lasers with flashlamps.

- *Related work by others*

Subsequent to our initial discovery, two groups of researchers found additional organic molecules with which laser-pumped stimulated emission could be achieved. When the present paper was essentially complete, we were made aware of the work of Schäfer, Schmidt, and Volze,[3] who, independently of us, observed and studied ruby-laser-pumped stimulated emission in several photosensitizing dyes, including 3,3′-diethylthiatricarbocyanine bromide (hereafter, DTTC bromide) and 3,3′-diethylthiadicarbocyanine iodide (hereafter, DTDC iodide). The DTTC bromide is closely analogous to DTTC iodide, while the DTDC iodide is a simple vinylene homologue[4] of the DTTC iodide molecule. Among the observations made by Schäfer et al. were quite large spectral shifts in the position of the stimulated emission band of DTTC bromide with changes in the dye concentration. As will be seen in Sec. 4, such shifts are very similar to what we have observed with DTTC iodide. A point of dissimilarity, however, is that Schäfer et al.[3] did not make use of an end-pumping arrangement, and in consequence, the conversion efficiencies and beam divergences they report are not as impressive as those we have observed with end-pumping.

A few days after we learned of the work by Schäfer et al., a publication by Spaeth and Bortfeld[5] reported observations of stimulated emission from the following polymethine dyes: 1,1′-diethyl-2,2′-dicarbocyanine iodide (referred to as "DDI" and 1,1′-diethyl-4,4′-carbocyanine iodide (cryptocyanine). Among the features of the stimulated emission observed by Spaeth and Bortfeld were shifts due to self-absorption. The dyes they studied were pumped in a transverse configuration and displayed higher pumping thresholds (20-40 MW) than the dyes studied in the present paper (0.1-1.0 MW). Thus, results achieved by various investigators now attest quite strongly that the class of organic dye lasers is a broad one.

2. Solvent effects

- *Solvent effects—DTTC iodide*

Of the two dyes considered in this paper, DTTC iodide was found to be much more soluble in ordinary organic solvents than was CAP. Specifically, DTTC iodide was very soluble in ethyl and methyl alcohol, acetone, n,n′-dimethylformamide (DMF), dimethyl sulfoxide (DMSO), 1-propanol, butyl alcohol, glycerin, and ethylene glycol. With the apparatus shown in Fig. 2, stimulated emission was obtained in the case of every one of these solutions. The spectra are shown in Fig. 3.

The exact procedure used in obtaining the spectra of Fig. 3 was as follows. The concentration of DTTC iodide in each solvent was adjusted to give a 30-percent low-level transmission at 0.694μ in a one-inch path length. (This roughly corresponds to a concentration of 10^{-5} moles/liter.) For the mirror common to both primary and secondary cavities (that is, mirror M_1), we employed a 2-inch-diameter, multiple-dielectric coated window which reflected 99 percent at 0.81μ and transmitted 60 percent at 0.69μ. The secondary cavity output mirror (mirror M_2) transmitted 25 percent at 0.81μ and 15 percent at 0.69μ. All mirrors and optical surfaces were aligned by use of an autocollimator.

Figure 2 End-pumping arrangement used with the DTTC iodide laser. The dye concentration was adjusted in most instances to give a low-level transmission of 30% at 0.69μ in a 1-inch path length.

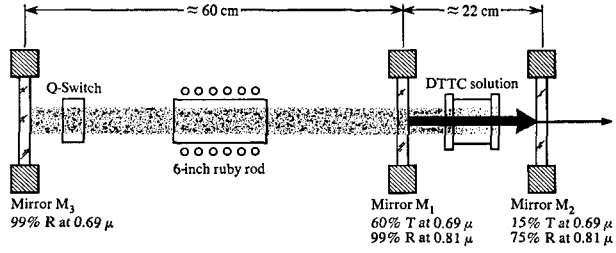

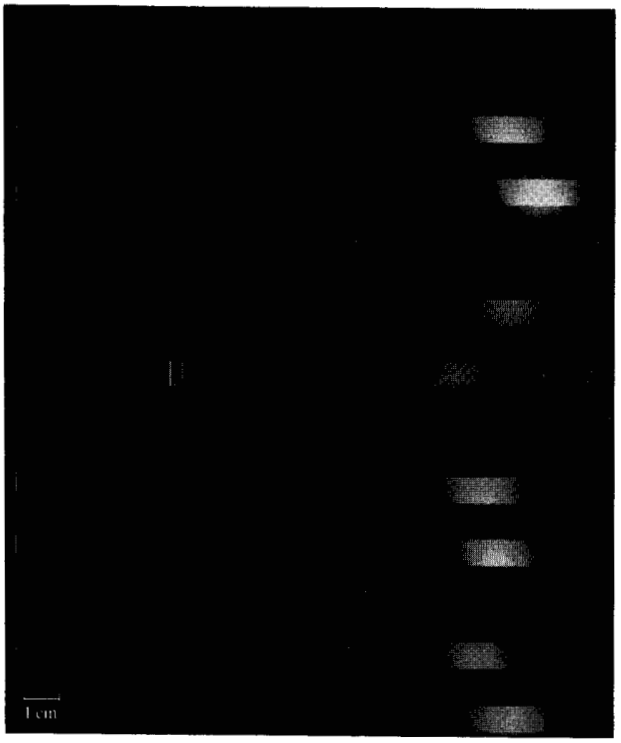

Figure 3 Stimulated emission spectra of DTTC iodide in nine solvents. The end-pumping arrangement of Fig. 2 was used here. Each solution was adjusted to transmit 30% at 0.69μ at low levels in a 1-inch path length. From top to bottom, the solvents are: glycerin, butyl alcohol, dimethyl sulfoxide, n,n'-dimethyl formamide, methyl alcohol, ethyl alcohol, l-propanol, acetone, and ethylene glycol. The 6943Å ruby laser line is recorded at the left. The dispersion of the spectrograph used was 8Å/mm. The entrance slit was set at 20 microns. The spectral lines used for calibration are mercury lines appearing in second order. A blue filter was used in the calibration process.

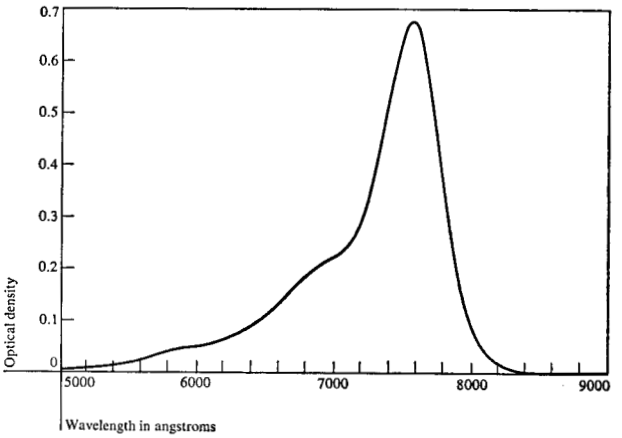

Figure 4 Absorption of DTTC in methyl alcohol. Optical density is plotted.

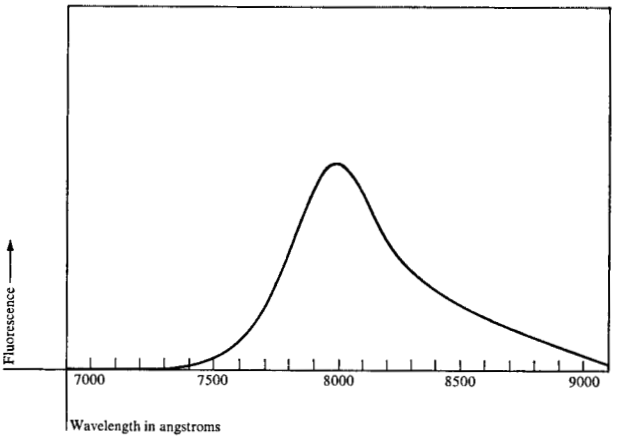

Figure 5 Fluorescence of DTTC in methyl alcohol, measured at low dye concentrations.

Stimulated emission spectra were photographed by directing the laser beam emerging from mirror M_2 onto the slit of a Bausch and Lomb grating spectrograph. The spectrograph was separated from the laser-pumped-laser by several feet so as to avoid any possibility that flashlamp light might be recorded on the plates. The dispersion of the grating used was 8Å/mm. The entrance slit of the spectrograph was set at 20μ. Focussing of the laser beam was not employed.

Each spectrum shown in Fig. 3 was produced with a single firing of the flashlamp that pumped the ruby laser.*

*At the condenser bank voltages employed (2800 V), four or five ruby laser giant pulses were usually produced, separated from one another by times on the order of 100 μsec. These giant pulses occurred simply because there was enough energy in the flashlamp to repump the ruby several times, and the vanadyl phthalocyanine passive Q-switch[6] used recovers in much less time than a microsecond. The output power of the largest of the 4 or 5 ruby laser giant pulses produced with each firing was usually about 25 MW. The mirror M_2 and the cell containing the DTTC iodide solution were both removed when making ruby laser power measurements.

It can be seen from Fig. 3 that the principal effect of varying the solvent is to shift the stimulated emission band, and that the width of the band remains about the same in each case. The approximate centers of the stimulated emission bands shown in Fig. 3 are as given in Table 1, together with the peak absorption and peak fluorescence wavelengths of DTTC iodide in each of the nine solvents tested. The values of λ_A given in Table 1 were obtained from absorption spectra similar to the one shown in Fig. 4. It will be noted that there is considerable absorption in the same spectral region in which stimulated emission occurs. This provides the basis for a simple explanation of the spectral shifts in the position of the DTTC iodide stimulated emission band that are observed to occur with changes in dye concentration in the regime of dilute solutions. (See Sec. 4).

A typical fluorescence spectrum observed for a DTTC iodide solution is plotted in Fig. 5, for which a 6328Å

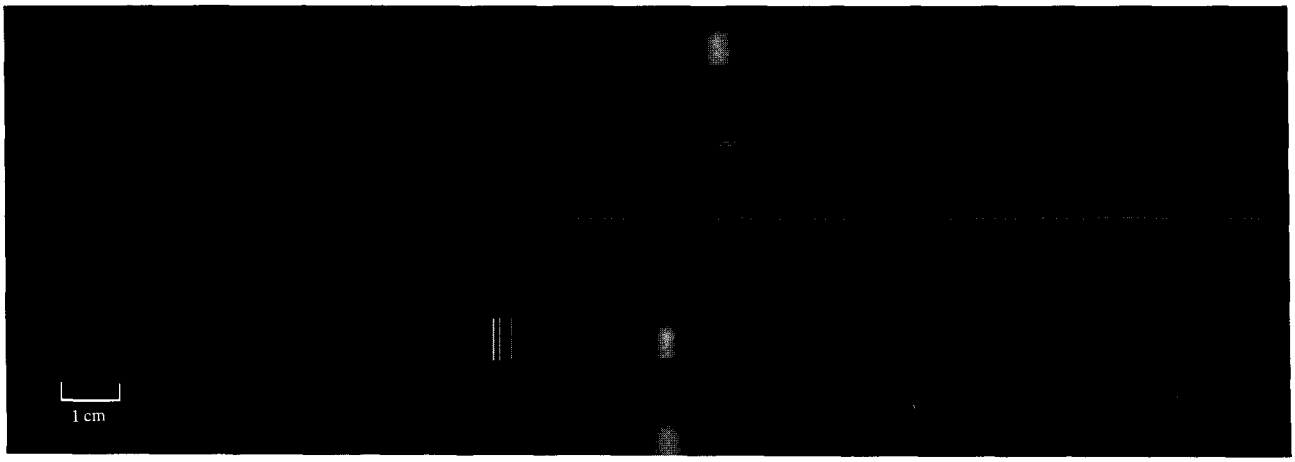

Figure 6 Stimulated emission spectra of CAP in four solvents. From top to bottom, DMSO, ethylene glycol, 1-propanol, and ethyl alcohol. The settings of the spectrograph are exactly the same as in Fig. 3. The transverse pumping arrangement of Fig. 1 was used here.

He-Ne laser was used to excite the fluorescence. It was from such traces that we obtained the values λ_F in Table 1. A discussion of the relationship of fluorescence spectra to the stimulated emission spectra will be found in Sec. 3.

• *Solvent effects—CAP*

In addition to being quite soluble in ethyl alcohol, CAP was found to dissolve rather easily in dimethyl sulfoxide, ethylene glycol, 1-propanol, methyl alcohol, and glycerin. Stimulated emission was observed in the case of four of these solvents, using the transverse pumping configuration shown in Fig. 1. Ruby laser pulses up to 10 MW were applied, and the length of the dye-containing cells employed was about one inch. The spectra are shown in Fig. 6. The CAP dye concentration generally found to give the best results displayed a low level transmission of about 20% at 0.694μ in a 1-mm path length; this corresponds to a concentration of about 10^{-3} moles/liter. End-pumping was not successfully realized with any of the CAP solutions, primarily because our mirrors did not discriminate well enough between the pump-source wavelength (0.694μ) and the CAP stimulated emission wavelength (0.755μ).

When one compares Figures 3 and 6, it is seen that the stimulated emission bands for CAP are less wide than those for DTTC iodide. The centers of the CAP bands roughly coincide with the positions occupied by the maxima of the most prominent vibronic fluorescence bands, Table 2. (In Table 2, the values of λ_A and λ_F were obtained from traces similar to those in Figs. 7 and 8).

For methyl alcohol, the CAP absorption and fluorescence spectra appeared practically the same as those for ethyl alcohol and, further, the luminescent quantum efficiency appeared to be about the same. However, for reasons unknown to us it was not possible to produce CAP stimulated emission using methyl alcohol as solvent and, again, applying up to 10MW of ruby laser power. Likewise, no stimulated emission was observed using glycerin.

Table 1. Centers of stimulated emission (λ_S), wavelengths of maximum absorption (λ_A), and peak fluorescence wavelengths (λ_F), for DTTC iodide in nine solvents.

Solvent	λ_S, *in* Å[a]	λ_A, *in* Å	λ_F, *in* Å
Methyl alcohol	7960 ± 20	7570 ± 10	7985 ± 30
Acetone	8015 ± 10	7590 ± 10	8030 ± 30
Ethyl alcohol	8030 ± 20	7625 ± 10	8045 ± 30
1-propanol	8070 ± 20	7640 ± 10	8075 ± 30
Ethylene glycol	8080 ± 20	7660 ± 20	8120 ± 30
DMF	8080 ± 20	7660 ± 20	8120 ± 30
Glycerin	8095 ± 20	7750 ± 20	8150 ± 30
Butyl alcohol	8095 ± 20	7660 ± 10	8090 ± 30
DMSO	8160 ± 20	7725 ± 10	8140 ± 30

[a] End-pumping configuration employed here. Solution adjusted for 30% transmission at low levels at 0.69μ in a 1-inch path length.

Table 2. Centers of stimulated emission (λ_S), wavelengths of maximum absorption (λ_A), and centers of longest wavelength fluorescence band (λ_F) for CAP in four solvents.

Solvent	λ_S, *in* Å[a]	λ_A, *in* Å	λ_F, *in* Å
1-propanol	7550 ± 5	6705 ± 10	7475 ± 10
Ethyl alcohol	7555 ± 5	6700 ± 10	7525 ± 10
DMSO	7615 ± 5	6770 ± 10	7575 ± 10
Ethylene glycol	7630 ± 5	6815 ± 10	7625 ± 10

[a] Transverse pumping configuration employed here.

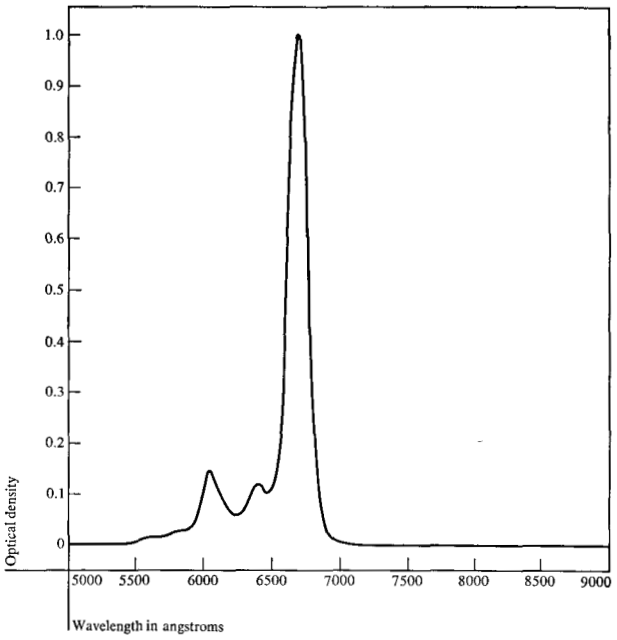

Figure 7 Absorption spectrum of CAP in ethyl alcohol. Optical density is plotted here.

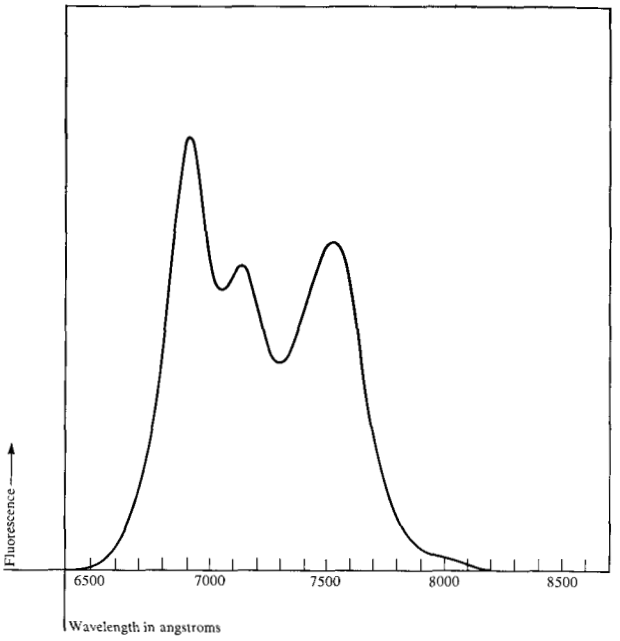

Figure 8 Fluorescence of CAP in ethyl alcohol.

Several attempts were also made, again without success, to obtain stimulated emission from magnesium phthalocyanine. The solvents tried were ethyl alcohol, pyridine, and acetone. This negative result is also rather puzzling, for the spectral characteristics of magnesium and chloroaluminum phthalocyanine appear to be quite similar.

• *Solvents and solvent stability*

The solvents used with both the DTTC iodide and CAP dyes were all reagent grade, with the exception of the DMSO and the DMF, which were spectrograde. No special precautions were made to outgas the solutions or to seal them against the atmosphere. It was noticed that all solutions of DTTC iodide became much less absorptive after several minutes of exposure to the (white) light beam of an absorption spectrometer. Decomposition was also very noticeable in dilute DTTC iodide solutions in unprotected cells exposed to ambient light for twelve hours or so.* In seeming contrast, exposure to the ruby beam for literally dozens of shots made within a few hours did not appear to affect the solutions adversely.

The CAP solutions, on the other hand, appeared to be very stable. For example, dilute solutions of CAP in ethyl alcohol which had been kept for several weeks without any particular concern for lightshielding could be made to lase as easily as freshly prepared solutions.

The DTTC iodide dye used was obtained from the Gallard-Schlesinger Chemical Mfg. Corp. of New York. The CAP dye was from a quantity prepared at IBM about three years ago.[6]

3. Energy level interpretations of the stimulated emission

• *Energy levels—CAP*

The simplified energy level diagram shown in Fig. 9 can be used to explain the lasing action observed in the case of the CAP dye. For definiteness, let us consider the case of ethyl alcohol solvent. From Table 2 and also from Fig. 7, the peak CAP absorption occurs at 6700 Å ($\sim$14 910 cm^{-1}). That value is represented in Fig. 9 as the distance between the lowest vibrational-rotational band ($v'' = 0$) of the ground electronic state and the lowest vibrational-rotational band ($v' = 0$) of the first excited (singlet) electronic state. The most prominent vibronic sideband in absorption occurs, from inspection of Fig. 7, at about 6040Å or, roughly, 16580 cm^{-1}. This energy determines the position of the vibrational-rotational band ($v'=1$) in Fig. 9. The separation between bands ($v'=0$) and ($v'=1$) is, therefore, about 1670 cm^{-1}. If we assume that the vibrational energy level separation in the ground electronic state is the same as in the excited electronic state, the separation

*Because of their ease of preparation, it was our practice to use fresh solutions of DTTC iodide. However, it is probable that one could preserve the lasing ability of the mixed solutions for longer periods of time by shielding the DTTC iodide from ambient light.

between bands ($v''=0$) and ($v''=1$) will also be about 1670 cm^{-1}. Then the peak of the fluorescent vibronic transition ($v'=0 \rightarrow v''=1$) should occur at 13240 cm^{-1} or, roughly, 7540 Å, assuming no large Franck-Condon shift. (The uniquely narrow singlet-singlet transitions of the phthalocyanine molecule result from this lack of a large Franck-Condon shift. Kosonocky, Harrison, and Stander[7] estimate this shift to be only some 60-80 Å.) The closeness of this deduced value (7540 Å) to the observed value of λ_F (7525 Å) suggests that the above discussion is roughly correct. That the principal CAP fluorescence band in Fig. 8 seems to occur at 6920 Å and not at 6720—6740 Å can be simply explained on the basis of self-absorption.

From Fig. 7 it is apparent that the ruby laser wavelength occurs at the very edge of the (0,0) absorption band. Thus the band of states ($v' = 0$) is directly populated by the ruby laser beam and an inversion is created in the (0,1) transition. From Table 2, the center of the stimulated emission band is seen to coincide almost exactly with λ_F in the case of ethylene glycol solvent. It does occur at slightly greater wavelengths for the other solvents, especially for 1-propanol, where it is definitely off the fluorescence peak. This displacement could be caused by the fact that at the dye concentrations employed in these experiments ($\sim 10^{-3}$ moles/liter) there is noticeable (although rapidly falling) absorption extending down to the region 7300—7700 Å, when measurements are made over a 1-in. path length. For the ethyl alcohol-CAP laser solution, as an example, the transmission in a 1-in. path length was measured to be as follows: at 7650 Å, 58%; at 7550 Å, 53%; at 7450 Å, 45%; and at 7350 Å, 37%. It is thus plausible that the laser frequency is simply displaced so as to obtain a more favorable gain-versus-loss situation. On the other hand, the presence of dimers in solution could produce the same effect (see Sec. 4).

On the whole, then, we believe that to picture stimulated emission in CAP as occurring via the (0,1) transition is to make a reasonable first approximation. In all likelihood, the states in the terminal band ($v'' = 1$) are very rapidly depopulated by non-radiative transitions of the CAP molecule, the process perhaps being induced by interactions with the surrounding molecules.

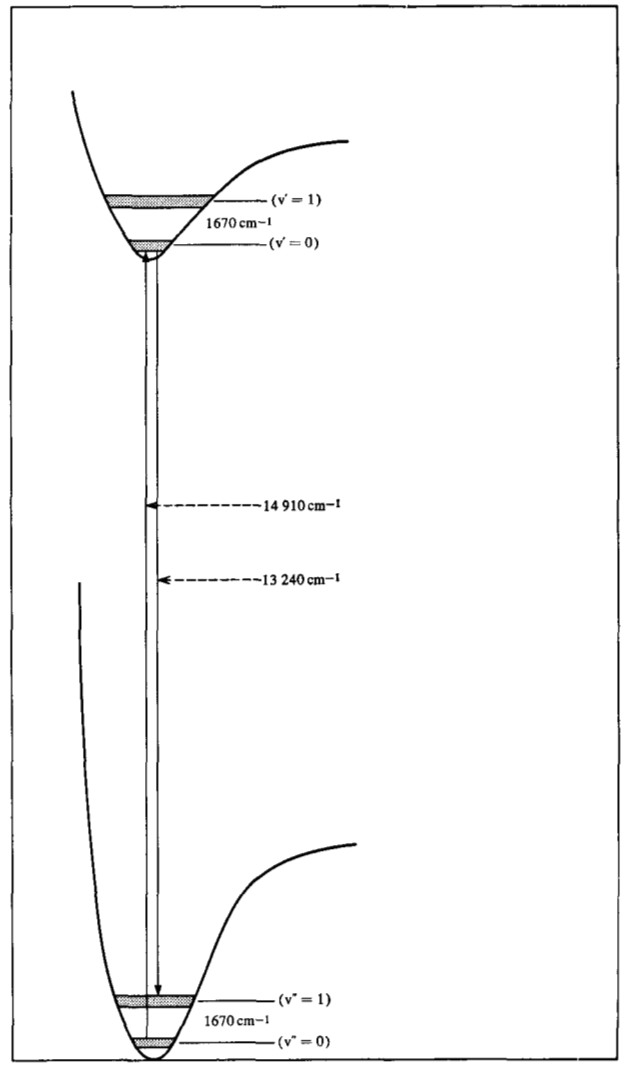

Figure 9 Energy level diagram for the CAP laser. The numbers refer to ethyl alcohol solvent. Potential energy is plotted vertically, while the abscissa represents a generalized configurational coordinate.

• *Energy levels—DTTC iodide*

In the case of DTTC iodide a somewhat different situation prevails, Fig. 10. There is evidence of a sizeable shift due to the Franck-Condon principle. The peak absorption occurs (in methyl alcohol solvent) at 7570 Å (13 190cm^{-1}). The peak fluorescence (again, in methyl alcohol) occurs at 7985 Å (12 510cm^{-1}). The appearance of the fluorescence band does not vary much with large changes in dye concentration, at least at the low concentration end of the scale, and that fact strongly suggests that its shape, measured at low concentrations (Fig. 5), is not seriously affected by self-absorption. One thus deduces the existence of a shift due to the Franck-Condon effect of some 680 cm^{-1} or so, and that deduction is supported by the fact that the widths of the optical transitions of DTTC iodide (Fig. 4) are much greater than those of CAP (Fig. 7).

The ruby laser wavelength appears to coincide (Fig. 4) with the maximum of the DTTC iodide vibronic absorption band ($v'' = 0 \rightarrow v' = 1$), and it also overlaps the tail of the (0,0) absorption band. Due to rapid non-radiative transitions in the excited electronic state, the end-effect of the ruby laser beam is to populate the vibrational-rotational band ($v' = 0$). At low dye concentrations stimulated emission in DTTC iodide occurs near the maximum of the (0,0) emission band, which is shifted away

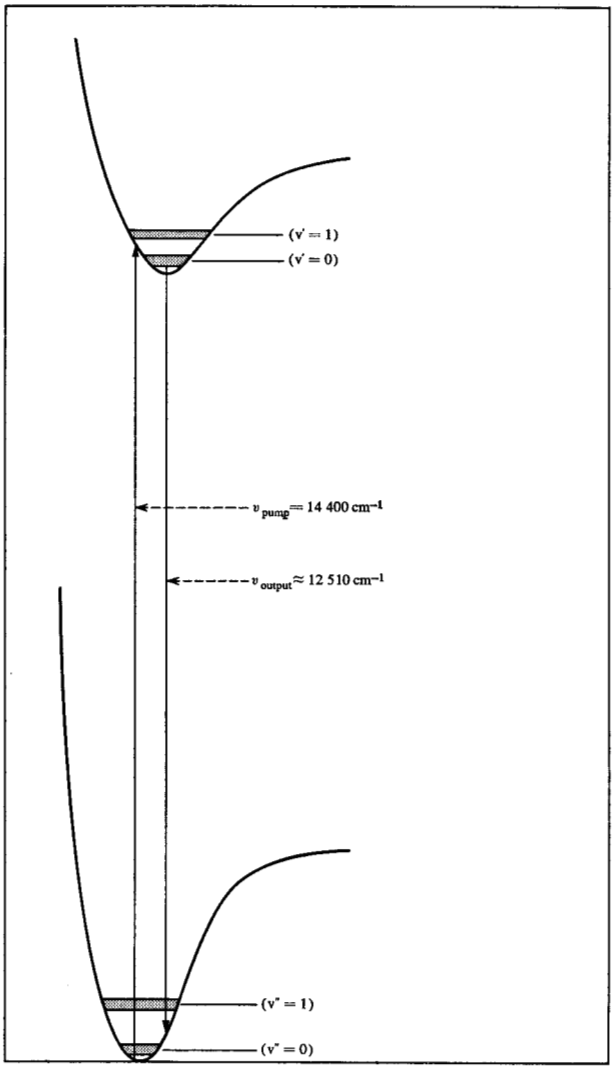

Figure 10 Energy level diagram for the DTTC iodide laser showing pumping and lasing transitions. Potential energy is plotted vertically, while the abscissa represents a generalized configurational coordinate.

from the maximum of the (0,0) absorption band by virtue of the Franck-Condon principle, as we have mentioned. Because of this shift, the effect of self-absorption on the lasing action is minimized. [With increasing concentrations, the stimulated emission band moves to longer wavelengths (Sec. 4), a result, most probably, of increasing self-absorption at the monomer fluorescence peak at low concentrations, and of dimer formation and energy transfer involving the latter at the highest concentrations.] For molecules generally, the ($v' = 0, v' = 1$) spacing very often differs from the ($v'' = 0, v'' = 1$) spacing when there is a sizeable shift arising from the Franck-Condon principle. The authors of Ref. 5 also point out the importance of Franck-Condon shifts in the laser systems they studied.

4. The DTTC iodide stimulated emission band: Shifts with variation in concentration

After initial experimentation, it soon became apparent to us that stimulated emission in DTTC iodide could be made to occur over a considerable range of dye concentration. Furthermore, large shifts in the spectral position of the lasing band were seen to accompany changes in the concentration of the dye solution. This same observation was independently noted by the authors of Ref. 3, who studied DTTC bromide quite carefully from this standpoint. Likewise, the authors of Ref. 5 also observed shifts in the spectra of their dyes.

Stimulated emission spectra of DTTC iodide in methyl alcohol for nine different dye concentrations are shown in Fig. 11, as obtained through use of the end pumping arrangement of Fig. 2. The strongest dye concentration allowing lasing to be achieved with that pumping arrangement (about 10^{-3} moles/liter) was observed to have a low-level 0.69μ transmission I/I_0 equal to 5% in a 1-mm path length. The laser spectrum corresponding to this concentration appears very weakly at the bottom of Fig. 11.

For each shot after the first the dye concentration was successively halved; thus, for the uppermost spectrum, the dye concentration has been reduced from the original value by a factor of 256. Then, at the ninth shot, after the concentration was halved once more, stimulated emission could no longer be achieved. From Beer's law, it follows that the solution corresponding to the top spectrum in Fig. 11 transmits 74 percent of incident low-level 0.69μ light in a one-inch path length. (The corresponding dye concentration is about 4×10^{-6} moles/liter). Note from Fig. 11 that the ruby beam is apparently completely absorbed at the higher dye concentrations employed. In contrast, polymethine dyes in low concentrations are used extensively for passive Q-switching of ruby lasers.[8,9]

The center of the stimulated emission band in the uppermost spectrum of Fig. 11 occurs at $\lambda = 7935 \pm 10$ Å. The stimulated emission band is seen to shift to longer wavelengths as the dye concentration is increased. At the strongest concentration allowing lasing to be achieved the center of the band occurs at $\lambda = 8465 \pm 20$ Å. Thus a total range of 530 Å is spanned by the shifting center of the lasing band. The value is reasonably close to the total shift (600 Å) observed by the authors of Ref. 3 for DTTC bromide in methyl alcohol, even though they employed a transverse pumping scheme.

The existence of a definite short wavelength limit for the position of the lasing band seems to be indicated by Fig. 11. According to the discussion in Sec. 3, this limit must correspond to the true peak of the main fluorescence band. The minimal center wavelength of the stimulated emission band for any of the nine solvents of Table 1 occurs at a somewhat shorter wavelength than the values of λ_S given in that table. The reason is that the stimulated emission

Figure 11 Stimulated emission spectra of DTTC iodide in methyl alcohol. The end-pumping configuration of Fig. 2 was used here. For the bottom spectrum (barely visible) the dye solution transmitted 5% at 0.69μ at low levels in a 1-mm path length. For each successive shot the dye concentration was halved. For the four top spectra the ruby laser line may be seen at the left. The other lines in the top spectrum are mercury lines appearing in second order. The grating dispersion is 8Å/mm. 50μ slits were used here.

spectra from which the values λ_S in Table 1 were derived were spectra that were obtained using solutions transmitting 30 percent at low levels. For DTTC iodide in DMSO, for example, the shortest wavelength for the center of the lasing band appears to be about 8120 Å, rather than the 8160 Å value listed for λ_S in Table 1.

Possible reasons for the effect of concentration on the lasing band position have already been mentioned in the previous section. With increasing concentration there appears increasing absorption at the fluorescence maximum, and the most favorable gain-versus-loss position is shifted towards longer wavelengths. This, we believe, is the principal reason for the observed shifts at low concentrations. On the other hand, at concentrations approaching 10^{-3} moles/liter, dye molecules are known to aggregate in solution, with the usual result that fluoresence maxima are shifted to longer wavelengths. Intermolecular energy transfer can lead to excited dimer state formation and thus to enchanced long-wavelength fluorescence emission. The relative importance of each of the two effects remains to be established.

5. The DTTC iodide laser: Conversion efficiency using the end-pumped configuration

- *Solvent variation and conversion efficiency*

The output of the DTTC laser from the end-pumped configuration of Fig. 2 was measured for each of the nine solvents listed in Table 1. Each solution was adjusted for a thirty-percent low-level 0.69μ-transmission in a 1-in. path length. Laser beam intensities were measured by a calibrated photodiode detector (S-1 response), used in conjunction with a Tektronix 519 travelling wave oscilloscope. The large attenuation required was provided by aqueous solutions of copper sulfate of known concentration, full account being taken of the wavelength dependence of the molar absorptivity. Several No. 7-69 Corning glass filters were also employed. These filters strongly block ruby laser light but allow light at $\sim$0.8μ to be relatively unattenuated.

It was found that the conversion efficiency of the DTTC iodide laser was highest in DMSO solvent. A peak beam intensity at $\sim$0.8μ of 6.1 MW was obtained using freshly prepared DTTC iodide-in-DMSO solutions adjusted for 30-percent transmittance at 0.69μ in a 1-in. path length. The secondary cavity output mirror M_2 and the dye-containing cell were then removed, and the intensity of the ruby laser pumping pulse was measured. This value was about 25 MW. In measuring the power of the ruby laser the same photodiode detector was used, but the concentration of the $CuSO_4$ solution was appropriately increased since ϵ, the molar absorptivity of $CuSO_4$ dissolved in water, is only about 6.5 at 0.69μ, whereas it is close to 12.5 at 0.81μ. For the ruby laser power measurement the Corning No. 7-69 filters were removed, of course. It is believed that the value of 25 percent for the conversion efficiency, obtained in the manner just described, is reasonably close to the true value.

The same procedure was followed for the eight other solvents. The measured conversion efficiencies are tabulated in Table 3. At present, the relationship between

Table 3. Conversion efficiencies for the DTTC iodide laser*

Solvent	*Conversion Efficiency, %*
Methyl alcohol	9.0
Acetone	7.0
Ethyl alcohol	6.5
1-propanol	11.5
Ethylene glycol	14.0
DMF	15.5
Glycerin	15.5
Butyl alcohol	9.0
DMSO	25.0

* The end-pumping configuration was employed here. Each solution was adjusted to give a 30% transmission at 0.69μ in a 1-inch path length at low levels. Estimated accuracy is 10% for each efficiency shown.

stimulated emission conversion efficiency and the usual quantum efficiency measured for fluorescent solutions[10] is not exactly clear to us. The exact reasons for the striking superiority of DMSO as a solvent are also unknown to us.

• *Concentration variation and conversion efficiency*

The conversion efficiency of DTTC iodide in DMSO was measured next as a function of dye concentration. It displayed only a moderate variation over the entire concentration range. For dye concentrations which transmitted at low light levels more than 50% at 0.69μ in a 1-in. path length the efficiency was less than for concentrations in the 10 to 50% transmission range, a range over which the efficiency was found to be roughly constant. For more concentrated solutions, however, the efficiency increased; it was found to be roughly 33 percent for dye concentrations transmitting only a few percent at 0.69μ in a 1-in. path length. For dye concentrations transmitting at 0.69μ only a few percent in a 1-cm path length the conversion efficiencies were still larger, close to 50 percent; they remained near this value for all further increases in dye concentration until, finally, the laser ceased to oscillate.

6. Transient response

Provided a computer is available, an organic dye laser, optically pumped by a giant pulse laser, is a relatively simple system to analyze from the standpoint of transients.[11] Having access to an IBM 7090/94, we undertook to use it in comparing the observed shapes of dye-laser output pulses with shapes produced by the computer as plots of solutions to the rate equations. Only the CAP laser system was studied in detail, for a theoretical analysis applicable to the case of DTTC iodide would be necessarily complicated by the presence of self-absorption (see Secs. 3 and 4) and the rate equations we employed were not explicitly written to take self-absorption into account. Nonetheless, a few measurements of DTTC iodide end-pumped laser output pulses were made.

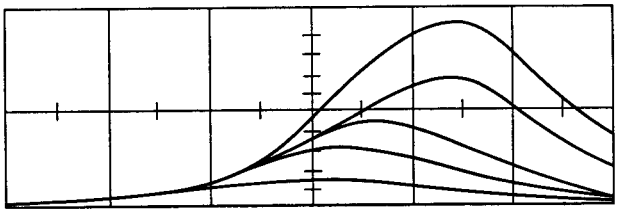

Figure 12 Typical ruby laser pulses used to pump the CAP laser. Scale, 10 nsec/div.

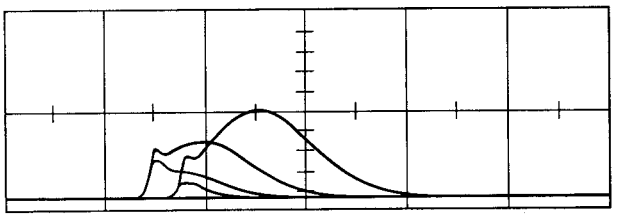

Fig. 13 Oscilloscope traces of the CAP laser, pumped in the transverse geometry. Mirror spacing, 5 cm. Mirror reflectivities at 0.755μ, 98% and 80%. Sweep speed, 20 nsec per main division.

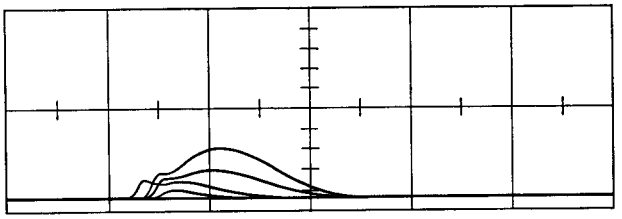

Figure 14 Oscilloscope traces of the CAP laser, pumped in the transverse geometry. Mirror spacing, 5 cm. Mirror reflectivities, both 98% at 0.755μ. Sweep speed, 20 nsec/div. Detector attenuation is one-tenth that in Fig. 13.

• *Experimental measurements*

The output beam of the CAP laser, pumped in the transverse geometry, was observed with a TRG 105B photodiode detector (S-20 response), used in conjuction with a Tektronix 519 travelling-wave oscilloscope. According to the manufacturers' specifications, the response time of the detector is better than 0.3 nsec and the rise time of the oscilloscope is 0.3 nsec. The detector was usually placed so as to intercept the beam from the secondary cavity directly. It was always covered by at least two No. 7-69 Corning glass filters so as to block out completely all scattered ruby laser light. Various additional filters were used to attenuate the CAP laser beam. To measure the shape of the ruby laser pulses (Fig. 12) the detector was repositioned and the No. 7-69 filters were removed. Various output mirrors were employed for the secondary cavity; the mirror separation, however, was kept constant at 5 cm. The dye concentration was also kept fixed.

Measurements of the output of the CAP laser, pumped by the series of four or five ruby laser pulses that occurred with each flashlamp firing, are shown in the typical oscilloscope traces of Figs. 13 and 14. The ruby laser pulses are shown in Fig. 12.

In the case, Fig. 13, of the more lossy cavity (i.e., the cavity with the lower-reflectivity mirrors) one notes that the phthalocyanine laser output rises rapidly, reaches an initial peak in 2—3 nanoseconds, then drops off, and ultimately appears to display a time variation roughly similar to the shape of the latter portion of the pumping pulse. The height of the initial spike appears to approach an asymptotic limit while the absolute maximum continues to increase with applied pumping power. For the case of the cavity with higher Q, Fig. 14, the risetime of the initial spike is much longer and the initial portions of the CAP laser pulses are, in general, less angular in character than for the more lossy cavity. By comparison of Figs. 12 and 13 it is seen that the risetime of the phthalocyanine laser can easily be shortened to 1/10 of the risetime of the primary ruby beam.

From the traces shown in Figs. 13 and 14 one can draw two conclusions: first, that lossy cavities are best for the generation of fast rising pulses; second, that for given cavity losses there is an optimum pump power, for too much pump power results in a pulse that substantially reflects the shape of the primary pulse, one having only a relatively small (albeit sharp) step at the beginning. (Both of the statements above will be fortified by the computer calculations that follow in the next section.)

The output of the DTTC laser, operated in the end-pumped configuration, was also examined. It appeared to mirror the shape of the pumping pulse, and displayed no sharply rising initial step. Possibly the presence of self-absorption accounts for this behavior. More work is needed to clarify the transient characteristics for this case.

- *Computer Solutions of the Rate Equations*

D. Roess has theoretically investigated the transient behavior of an optically pumped system by treating numerical examples with a digital computer.[11] In his paper, however, it is assumed that the duration of the pumping pulse is short compared to the spontaneous emission decay time. The terms representing spontaneous emission decay were omitted in Ref. 11 from the rate equations. Because the radiative decay times of singlet-singlet transitions of organic dye molecules are known to lie in the 1 to 10-nsec range, and the ruby laser pumping pulses employed in our experiments were at least 20 nsec wide (Fig. 12), we concluded that in our case we could not neglect spontaneous emission decay. Therefore, we sought computer solutions that would take it into account explicitly.

We studied the following mutually coupled rate equations:

$$\frac{dn}{dt} = W(t) - \frac{n}{n_0}\frac{q}{t_c} - \frac{n}{\tau}, \tag{1}$$

$$\frac{dq}{dt} = \frac{q}{t_c}\left(\frac{n}{n_0} - 1\right). \tag{2}$$

Equations (1) and (2) differ from those of Ref. 11 only by the addition of the term n/τ (to the first equation). The quantities appearing in the above are as follows: n is the inversion ($n = n_2 - n_1 \sim n_2$); n_0, the threshold inversion; q, the number of quanta in the cavity; t_c, the resonator lifetime; and τ, the fluorescence lifetime. W(t) is the pumping pulse; it is assumed to have a Gaussian distribution with half-width at half-power points equal to T_1,

$$W(t) = W_{\max} \exp\left[-\left\{\frac{t}{T_1}(\ln 2)^{1/2}\right\}^2\right]. \tag{3}$$

The total number of pumping photons is given by

$$\int_{-\infty}^{\infty} W(t)\, dt = N.$$

Unit fluorescent quantum efficiency is assumed. By defining new variables as follows,

$$y_1(t) = q(t)/(t_c W_{\max}), \tag{4a}$$

$$y_2(t) = n(t)/N, \tag{4b}$$

$$x = t/t_c; \tag{4c}$$

and defining a set of dimensionless parameters as follows,

$$\alpha = N/n_0, \tag{5a}$$

$$\beta = \tau/t_c, \tag{5b}$$

$$\gamma = T_1/t_c; \tag{5c}$$

we transform Eqs. (1) and (2) into Eqs. (6) and (7), whose form is suitable for machine computation:

$$\frac{dy_2(x)}{dx} = \frac{1}{\gamma}\left(\frac{\ln 2}{\pi}\right)^{1/2} \exp\left[-\left\{\frac{x}{\gamma}(\ln 2)^{1/2}\right\}^2\right] - \frac{\alpha}{\gamma}\left(\frac{\ln 2}{\pi}\right)^{1/2} y_1(x)y_2(x) - \frac{y_2(x)}{\beta}, \tag{6}$$

$$\frac{dy_1(x)}{dx} = y_1(x)[\alpha y_2(x) - 1]. \tag{7}$$

A variation of the Runge-Kutta method[12,13] was used to find numerical solutions of Eqs. (6) and (7) for various values of α, β, and γ. The step-by-step integration was performed in approximately 1000 steps over a range of values of x such that the exponential term did not exceed $e^{88.028}$ (so as to remain within the bounds of our computational technique).

To begin the computations, it was necessary to assume a finite initial value of y_1 (1×10^{-9}). The assumption insures a non-trivial solution and corresponds, physically, to the fact that photon noise is necessary to initiate the lasing process.

Examples of the computer solutions are shown in Figs. 15-31. We consider first the traces appearing in Figs. 15-25. These show solutions of Eqs. (6) and (7) for several values of α, the values of β and γ being fixed at 3 and 6, respectively. We invoke, as Eq. (8), the well-known formula for the cavity decay time on the grounds that it is applicable when the losses are primarily transmissive ones. Doing so, we have

$$t_c = n_r l/(1 - R)c, \tag{8}$$

where n_r is the refractive index of the medium occupying the (entire) space between the end mirrors; l is the separation between the end mirrors; and R is the geometrical mean, $R = (R_1R_2)^{\frac{1}{2}}$, of the end mirror reflectivities. When one substitutes into Eq. (8) the values $R = 0.886$, $l = 5$cm, and $n_r = 1.5$, which values apply in the case of Fig. 13, one obtains a value of t_c equal to 2.2 nsec. With $\beta = 3$ and $\gamma = 6$ this would imply a value of $\tau = 6.6$ nsec and a value of $T_1 = 13.2$ nsec. From Fig. 12 it is seen that the latter value is certainly a good choice, while the value of 6.6 nsec is a typical metal phthalocyanine fluorescence decay time.[14] Thus it is perhaps not surprising that the traces shown in Figs. 15-25 strongly resemble the traces of Fig. 13.

From Figs. 15-25, it can be seen that theoretically the amplitude of the initial spike should at first increase very rapidly with applied pumping power. However, the rate of growth of this spike should soon become subordinate to the rate of growth of the rest of the pulse. This phenomenon indeed appears to occur, judging by the traces shown in Fig. 13 where, for the largest pulse shown, the ratio of the height of the main pulse to the height of the initial step is seen to be roughly equal to 2. This particular pulse, therefore, would appear to correspond nearly to the case $\alpha = 350$ (Fig. 21). Let us see what this implies about the order of magnitude of the threshold inversion n_0. The number of photons N in a 10-MW, 20-nsec ruby laser pulse is roughly 7×10^{17}. Thus from Eq. (5a) the value of n_0 is deduced to be about 2×10^{15}. Roughly the same value is obtained by an independent calculation[1] of the CAP threshold inversion employing the well-known Townes-Schawlow formula.

We note in Fig. 24 the presence of a small second dip in the trace representing the time variation of the excited state population. This dip signals the beginning of a new spike or step, one which evidently should occur near the top of the pulse. In Fig. 25 the development of this additional step in the formal computer solutions has proceeded to the point where its appearance in the function $y_1(x)$ can be plainly observed. (In Fig. 25 we omit presentation of the associated function $y_2(x)$ because it takes on negative values during the second spike. The physical model upon which Eqs. (1) and (2) are based is that of a laser with infinitely fast-emptying terminal states; for such a laser $n(t)$ must always be greater than zero.) It would seem valid to deduce from Figs. 13, 21, 24, and 25, taken collectively, that a multi-stepped pulse might have been observable with the laser used to produce the traces of Fig. 13 if the pumping intensity had been increased to a value some $2\frac{1}{2}$ times greater than that corresponding to the largest pulse shown. On a few occasions, when somewhat different cavity parameters were involved, multi-stepped CAP laser pulses were actually seen.

Table 4. Calculated risetimes of the leading edge of the laser pulse. (The significance of quantities α, β, and γ is discussed on page 139.)

α	β	γ	t_c, *in nsec*	η_R, *in nsec*
50	3	6	2.2	1.01
75	3	6	2.2	0.9
100	3	6	2.2	0.79
350	3	6	2.2	0.66
600	3	6	2.2	0.66

The computer solutions can clearly be used to predict the risetime for the initial spike or step. It was primarily for this reason that we decided to examine the transient response theoretically. In Table 4 computer-predicted risetimes η_R are listed for some of the solutions shown in Figs. 15-25. (Risetime is here defined as the time required for the pulse to rise from 10 percent to 90 percent of its peak height. Only the initial portion of the pulse is considered.) The values η_R were obtained directly from the computer printout. For definiteness, the value of t_c in Table 4 was chosen to be the same as the value obtained earlier, i.e., the value based upon the cavity parameters of Fig. 13. Note that the fastest predicted risetime is about 0.7 nsec, and that the variation in η_R with pump power is not large. The risetimes actually measured from the original traces of Fig. 13 were in the neighborhood of 2 to 3 nanoseconds. The lack of any closer agreement may reflect that in actuality many modes are simultaneously excited.

We conclude this section by presenting several more traces (Figs. 26-31) depicting, again, computer solutions of Eqs. (6) and (7). Here the choice of parameters is $\beta = 0.6$ and $\gamma = 1.2$. Various values of α are represented. Figures 26-31 should more or less correspond to the experimental traces of Fig. 14. Using Eq. (8), a value $t_c = 12.5$ nsec is obtained; if we again assume τ and T_1 to be, respectively, 6.6 and 13.2 nsec the values of β and γ turn out to be 0.53

Figures 15-20 Examples of computer solutions to the rate equations discussed in the text.

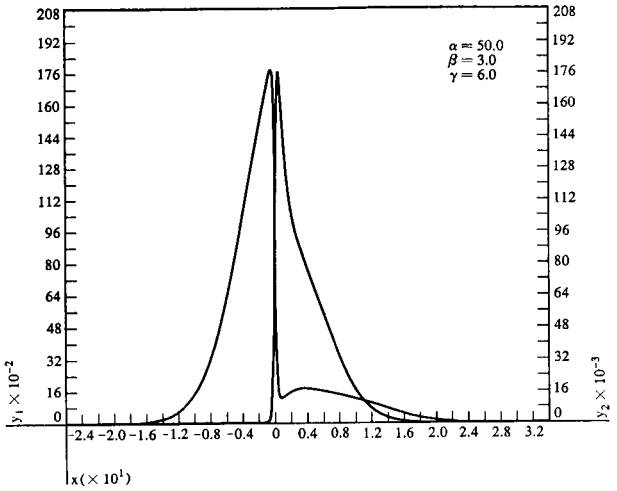

Figure 15

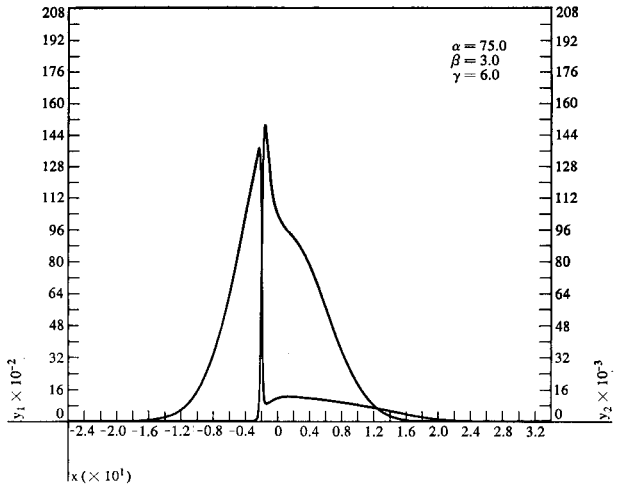

Figure 16

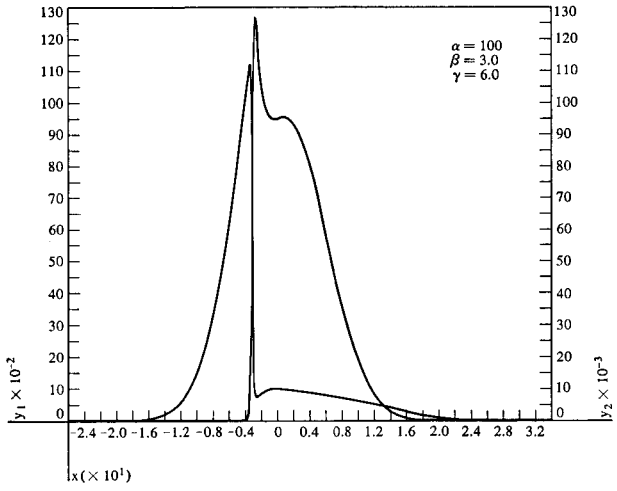

Figure 17

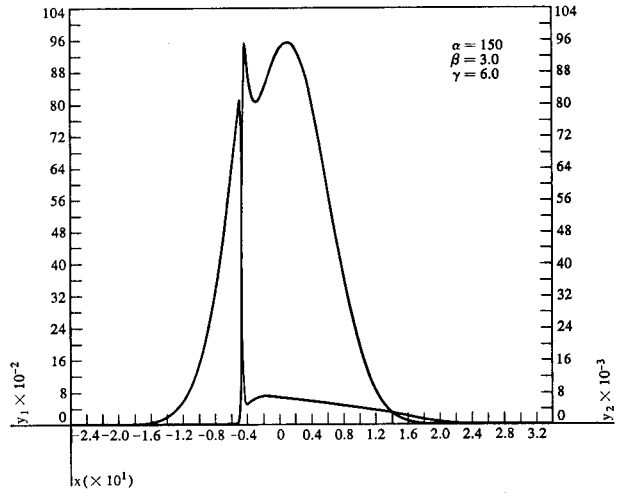

Figure 18

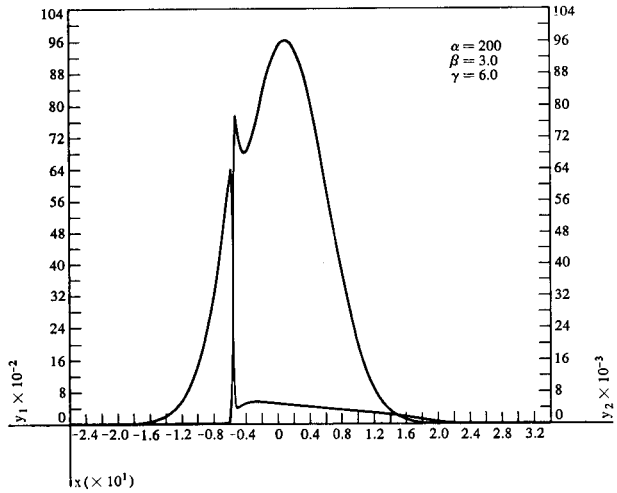

Figure 19

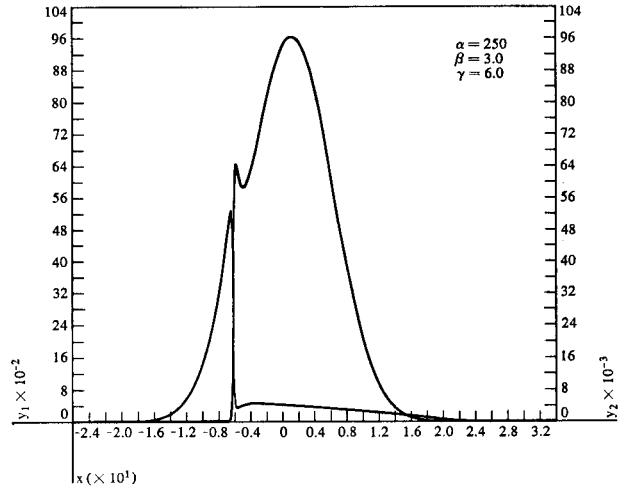

Figure 20

Figures 21-25 Further examples of computer solutions to the rate equations discussed in the text.

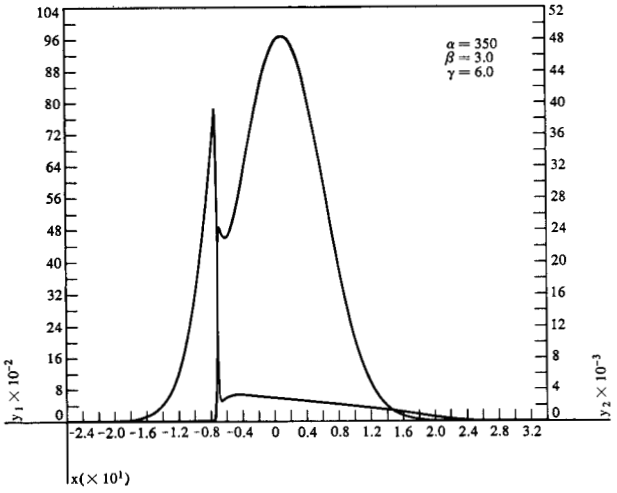

Figure 21

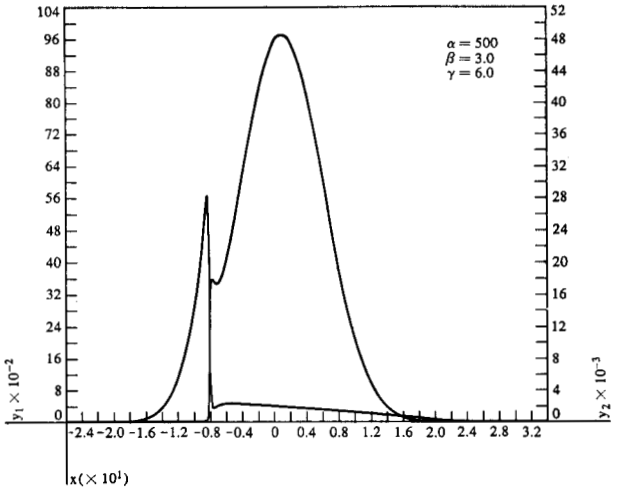

Figure 22

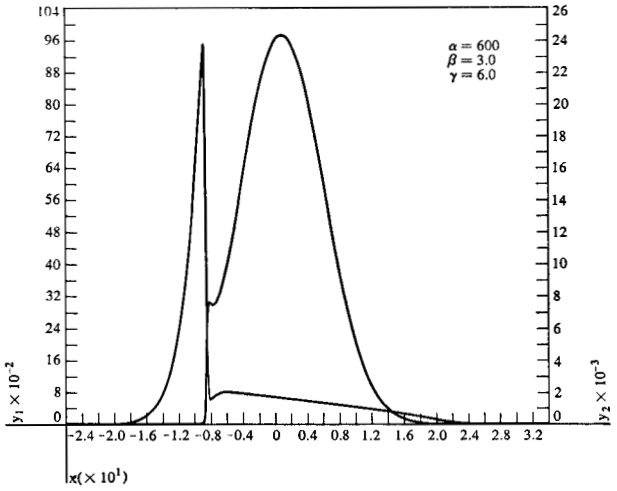

Figure 23

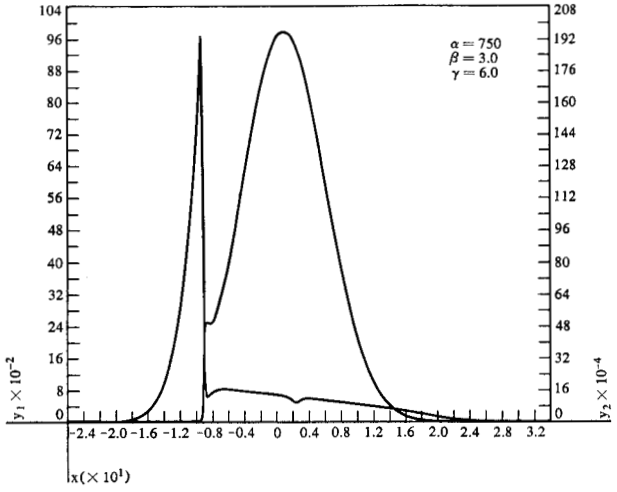

Figure 24

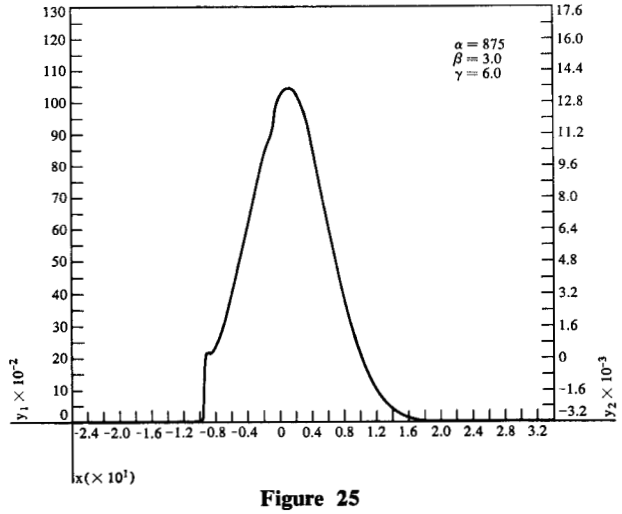

Figure 25

and 1.05, reasonably close to the values 0.6 and 1.2 assumed for Figs. 26-31. Generally speaking, the traces comprising Figs. 26-31 rise slower than those comprising Figs. 15-25 and it becomes difficult to isolate a leading edge in any case for which $\alpha < 150$. Even when the edge is fairly well defined—for instance, as in Fig. 30 where $\alpha = 500$—the risetime is not particularly short. For Fig. 30, the time for $y_1(x)$ to rise from 3×10^{-2} to 20×10^{-2} is 1.13 nsec, assuming a value of 12.5 nsec for t_c. Most of the risetimes involved in Figs. 26-31 are clearly much longer. The fact that the the risetimes of the traces in Figs. 26-31 are generally longer than those in Figs. 15-25 has its experimental counterpart in the fact that the risetimes of the traces in Fig. 14 are longer than those of the traces in Fig. 13. Clearly, in order to generate fast-rising pulses, a cavity with a large output coupling should be employed.

Figures 26-31 Further examples of computer solutions to the rate equations discussed in the text.

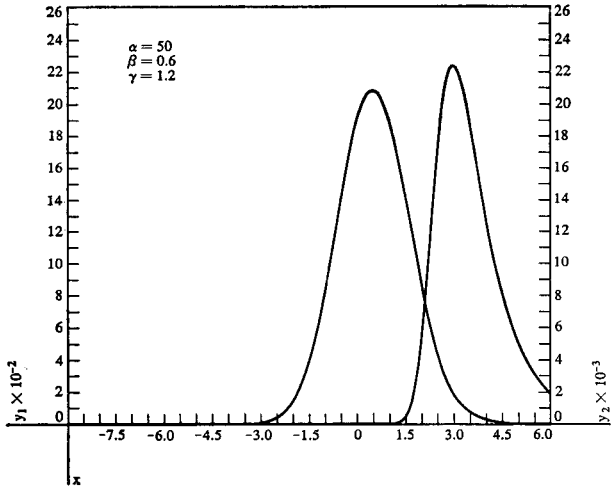

Figure 26

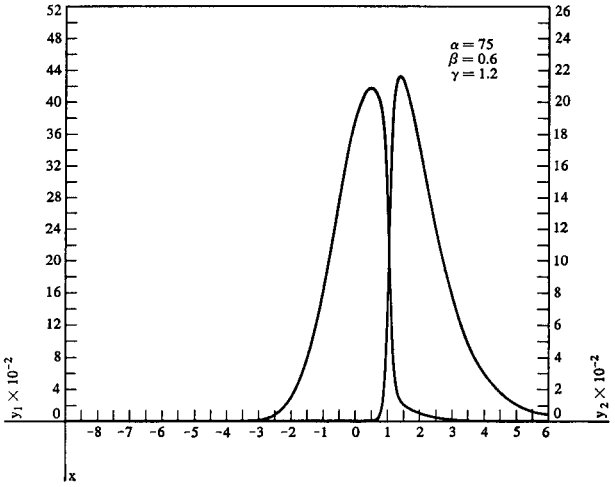

Figure 27

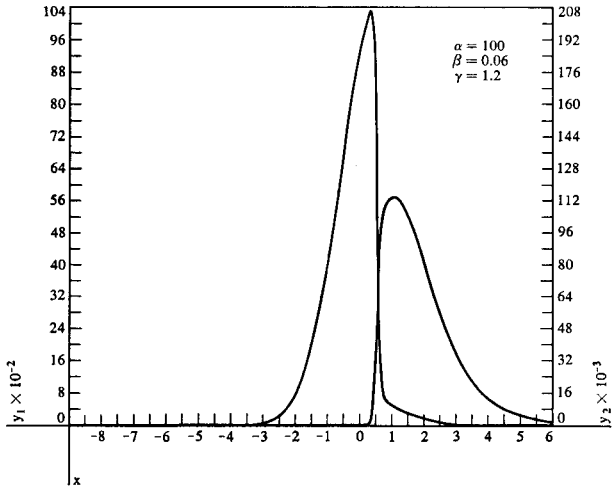

Figure 28

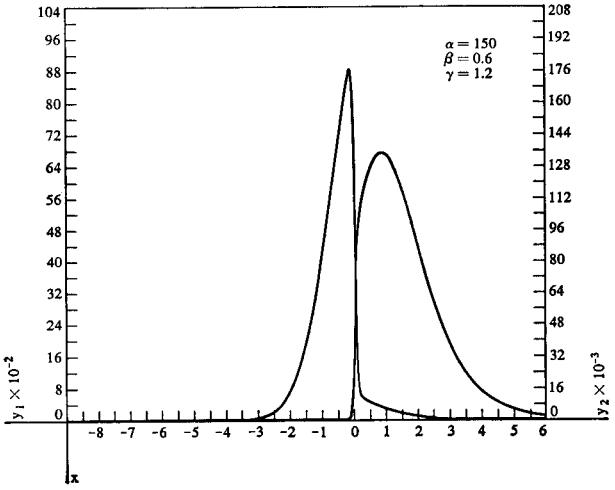

Figure 29

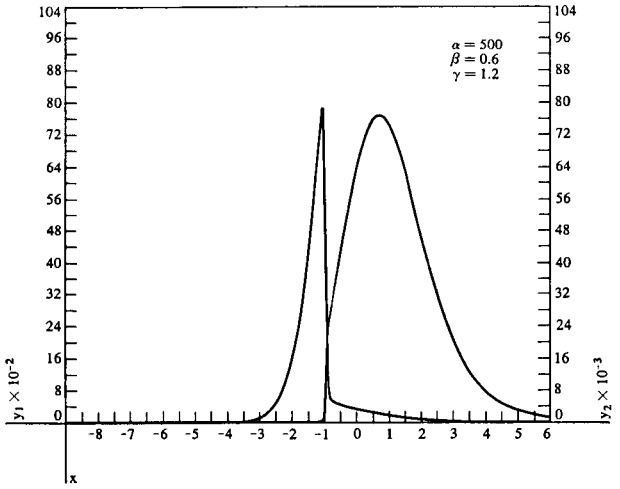

Figure 30

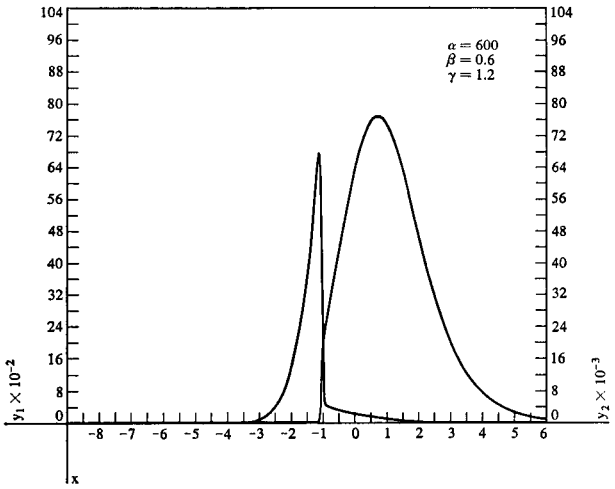

Figure 31

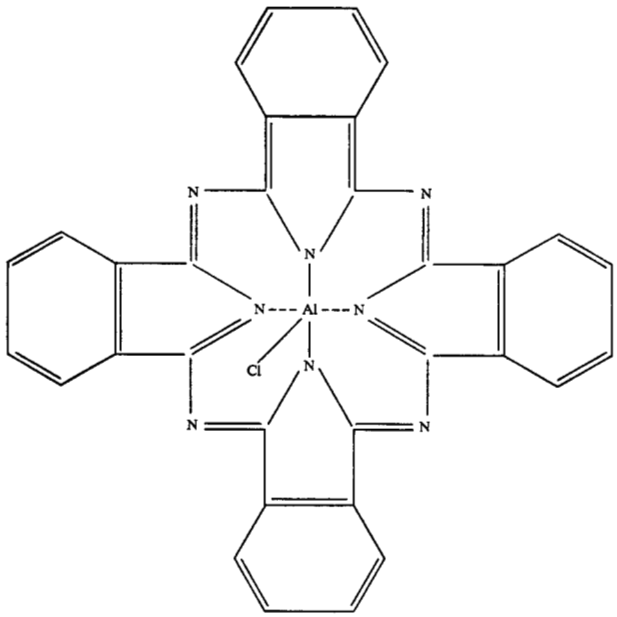

Figure 32 The chloro-aluminum phthalocyanine molecule.

7. Polarization effects

A divalent metal phthalocyanine molecule is planar, with square symmetry, Figure 32. For chloro-aluminum phthalocyanine, the charge-compensating Cl^- ion is probably located atop the central Al^{3+} ion, and the point group symmetry for the conjugated π-electron system may reasonably be taken as C_{4v}. However, since the spectral (i.e., absorption and fluorescence) characteristics of chloro-aluminum and magnesium phthalocyanine are virtually identical, there is no apparent harm in assuming D_{4h} symmetry. Then parity is a good quantum number.

The ground electronic state of the phthalocyanines must be totally symmetric (A_{1g}). It can be easily proven that the only transitions allowable in absorption from A_{1g} states in D_{4h} symmetry are those to E_u states. Thus the emitting state of the phthalocyanine laser must be a two-fold degenerate E_u state. The irreducible representation associated with the laser terminal state will depend upon the symmetry of the vibration involved. According to Ref. 15 the most likely irreducible representation for the terminal state is either B_{1g} or B_{2g}. In either case, the fluorescent transition has to be a σ_e (electric rotor) transition. The pumping transition also has to be a σ_e transition. That the spectral transitions of the phthalocyanine molecule involve σ_e rather than π_e (electric dipole) transitions is also suggested by Kuhn's model[16]; according to that model, the 18 π-electrons responsible for the optical properties of the molecule move in the closed loop generated by the alternate passage from a nitrogen to a carbon atom. See Fig. 32.

With the knowledge that both pump and laser transitions are electric rotor transitions, one can use Feofilov's analysis[17] to predict the preferred direction of polarization for the output beam. In Ref. 17 an isotropically oriented system of molecules is assumed, and the dependence of the intensity of spontaneous emission viewed at right angles to the direction of the exciting beam is given as a function of the angle η (Fig. 33) for the cases in which **(a)** both absorption and emission are by linear oscillators (π_e), **(b)** absorption is by π_e oscillators and emission is by σ_e rotors, and **(c)** both are by σ_e rotors. (The analysis assumes that no significant orientational depolarization occurs during the time of photon emission; this assumption would seem to be most valid when stimulated emission can be made to occur, i.e., as in the experiments described in this paper.)

As stated above, the case which must apply here is case **(c)**. For a (σ_e,σ_e) sequence, Feofilov gives the following formulae

$$I_z \sim \frac{4\pi}{15}(3 + \cos^2\eta), \qquad I_x \sim \frac{4\pi}{5}, \tag{9}$$

and

$$I_{\text{total}} \sim \frac{6 + \cos^2\eta}{7}. \tag{10}$$

From these equations it follows that **(a)** with a vertically polarized pumping beam, the phthalocyanine laser output beam should also be vertically polarized, at least near

Figure 33 Relationship of the propagation direction and polarization of the exciting light to the direction for observation of spontaneous emission assumed in Ref. 17.

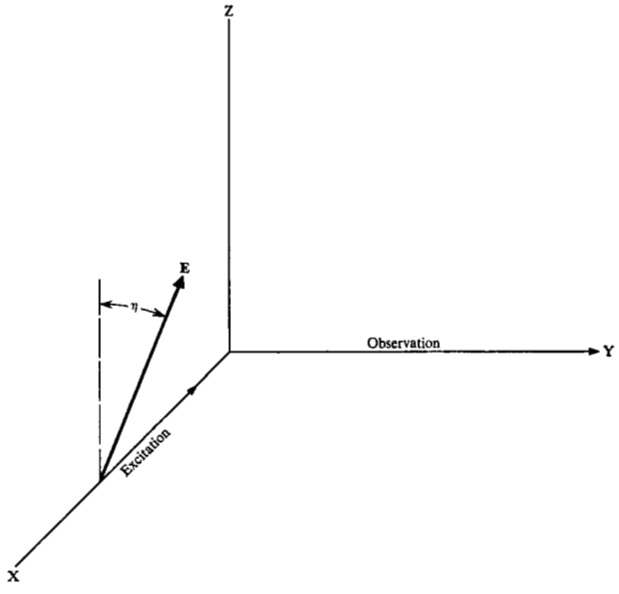

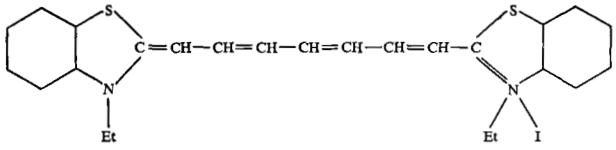

Figure 34 3,3'-diethylthiatricarbocyanine iodide molecule.

threshold, and that **(b)** the lasing threshold should be slightly lower for a vertically polarized pumping beam. Using a box-shaped cell we were (marginally) able to verify **(b)**. We also (marginally) succeeded in obtaining a predominantly vertically polarized output beam when the ruby beam was vertically polarized and its intensity was carefully regulated to be close to threshold. Thus experimental tests lend a little support to the (σ_e,σ_e) model. When the CAP laser was operated moderately above threshold, the output beam was observed to be unpolarized, again with the ruby beam vertically polarized. In view of the fact that the maximum value of the ratio I_z/I_x is only 4/3, this would normally be expected. On the other hand, it should be kept in mind that depolarization due to intermolecular energy transfer also would result in the same effect. At the dye concentrations employed here (about 10^{-3} moles/liter) energy transfer often starts to become important in other dye systems.

For (π_e,π_e) transitions the expressions analogous to Eqs. (9) and (10) are

$$I_z \sim \frac{2\pi}{15}(1 + 2\cos^2\eta), \qquad I_x \sim \frac{2\pi}{15} \tag{11}$$

and

$$I_{\text{total}} \sim \frac{1 + \cos^2\eta}{2}. \tag{12}$$

By inspection of Fig. 34 one clearly expects a (π_e,π_e) sequence in the case of the DTTC iodide laser. We indeed observed (very clearly) that when the DTTC laser was transversely pumped by a vertically polarized ruby beam, the output beam was vertically polarized, even for the highest pump powers applied. (A molar dye concentration of 10^{-5} was employed for these measurements). The DTTC iodide laser output beam was also observed to have the same polarization as that of the ruby laser when the end-pumping configuration was used. The more definitive character of the results observed in the case of DTTC iodide, as compared with those observed for CAP, may indeed reflect the absence of intermolecular energy transfer in the former system at the dye concentration employed (10^{-5} moles/liter).

For (π_e,σ_e) sequences the equations analogous to Eqs. (9)-(12) are

$$I_z \sim \frac{4\pi}{15}(1 + \sin^2\eta), \qquad I_x = \frac{8\pi}{15} \tag{13}$$

and

$$I_{\text{total}} \sim \frac{3 + \sin^2\eta}{4}. \tag{14}$$

Note that if a (π_e,σ_e) sequence were involved in either the CAP or the DTTC iodide case, the laser beam should be *horizontally* polarized when the pump light is vertically polarized.

8. Conclusion: The possibility of dye laser excitation by flashlamps

The preceding sections have amply demonstrated that laser-pumped stimulated emission may be achieved in the strongly allowed singlet-singlet transitions of organic molecules. Yet, the coherence possessed by the laser beam used for excitation is really non-essential. The truly important features of the ruby beam, insofar as its ability to pump the dye laser is concerned, are (a) its high peak intensity, and (b) its short risetime. Since the importance of the latter feature may not be as apparent as that of the former, it may be profitable to examine the situation. To obtain the fullest view, it will be productive to analyze the requirements for a flashlamp to be capable of exciting the dye laser.

Let us determine, first of all, the minimum light intensity that the flashlamp must supply to keep the dye laser on the verge of oscillation, i.e., the threshold pumping power. To do this, the well-known Townes-Schawlow formula for the required inversion density at threshold is written down,

$$n_i = 8\pi^2\tau\,\Delta\nu(1 - R)n_r^2/(\lambda_e^2 l\phi), \tag{15}$$

and parameters appropriate for the (DTTC iodide) laser are then substituted. In the above expression, l represents the active-region length; ϕ, the fluorescent quantum efficiency; $\Delta\nu$, the half width of the (assumed single) fluorescence band; τ, the observed lifetime of the fluorescence; n_r, the index of refraction; and R, the reflectivity of the end mirrors. Choosing the values $l = 10$ cm, $\phi = 0.1$, $R = 0.95$, and $\tau = 5$ nsec, and from Fig. 5 obtaining the values $\lambda_e = 0.8 \times 10^{-4}$cm, $\Delta\nu = 400 \times 3 \times 10^{10}$ Hz, we find that the resulting threshold inversion density n_i works out to be $\sim 10^{14}$ molecules/cm^3. The population density required in the first excited singlet state of DTTC iodide at threshold will be reasonably close to this number, because of the large Franck-Condon shift discussed in Sec. 3. We will take it to be the same. The minimum pumping power per-unit-volume required to maintain this inversion is $p = n_i h\nu_e/\tau$, or about 5kW/cm^3. Hence, for a 1-cm^2 cross section and a resonator 10 cm long, the total required pumping power is $P = 50$kW.

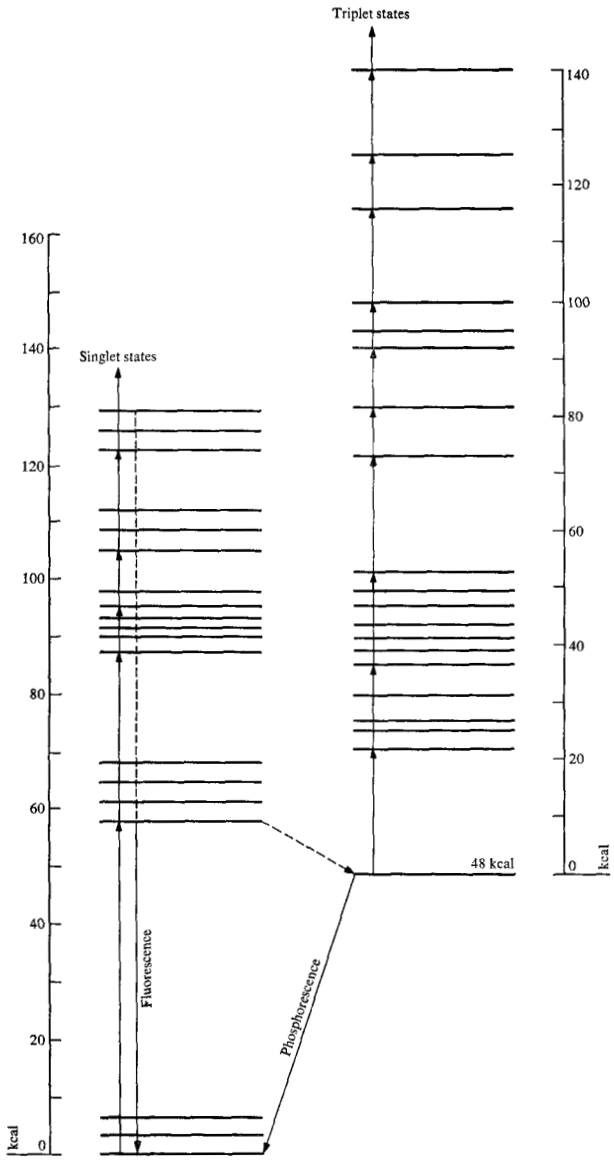

Figure 35 Singlet and triplet states of the Acridine Orange cation. (After Figure 7 of Ref. 18.)

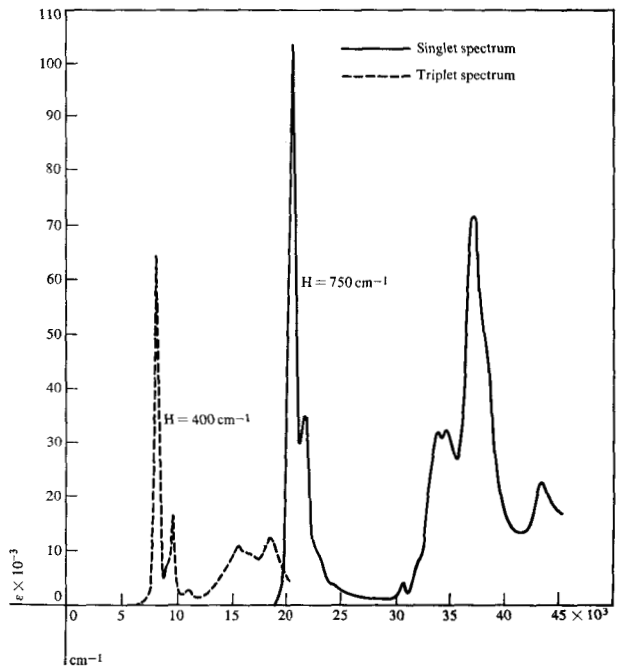

Figure 36 Singlet-singlet and triplet-triplet absorption spectra of the Acridine Orange cation at −183°C. (After Fig. 2 of Ref. 18.) Concentration, 10^{-4} molar; solvent, ether/alcohol (1:2); temperature, −183°C.

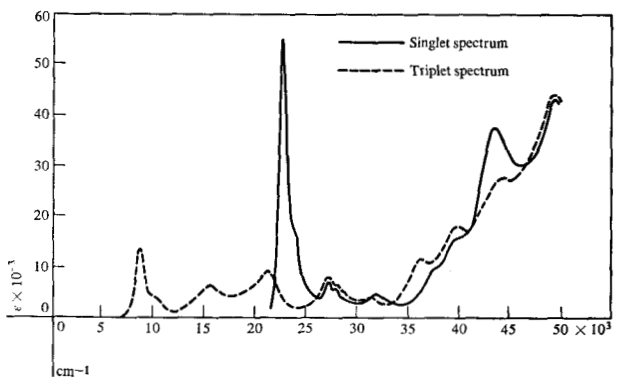

Figure 37 Singlet-singlet and triplet-triplet absorption spectra of the Fluorescein cation at −183°C. (After Fig. 5 of Ref. 19.) Concentration, 10^{-4} molar; solvent, ether/alcohol (1:2); temperature, −183°C.

The necessity for rapid pump excitation arises because a certain number of molecules will accumulate in the lowest triplet state, a metastable level, as a result of non-radiative decay from the lowest excited singlet state (Fig. 35) during the time required for the pumping flux to reach its peak. Transitions are, in general, strongly allowed from the lowest triplet state to higher triplet states, and these may occur in the same spectral region occupied by the singlet-singlet fluorescence peak. Thus the triplet state population density n_T accumulated by the time the first excited singlet state population density reaches the value n_i may, in fact, produce an over-all loss, so that no laser action is possible. Clearly, knowledge of the relative strengths of triplet-triplet and singlet-singlet transitions is very important in this connection. Although triplet-triplet spectra have been determined so far for only a relatively few organic molecules, excellent studies of this sort have been performed by Zanker and Miethke[18,19] for a number of dye molecules (see Figs. 36, 37). We will use their results as guidelines in what follows.

From Figs. 36 and 37 we roughly estimate that the absolute magnitude of the loss due to triplet-triplet absorptive transitions would be about one-tenth that of the gain due to singlet-singlet fluorescent transitions, at the frequency corresponding to the fluorescence peak, were there equal populations in the lowest triplet and first excited singlet states. (We here assume that the fluorescence peak occurs $\sim$ 1000 cm^{-1} to the long-wavelength side of the singlet-singlet absorption peak. We also note that the spectra in Fig. 36 and 37 represent data taken at $-$ 183°C; the room temperature spectra would be considerably broader and would produce more overlap.)

For definiteness, let us consider a pumping flux rising linearly with time, reaching its peak in, let us say, 0.5 μsec. Assuming that the peak lamp power corresponds to the threshold pump power P, the density n_T of molecules that will have accumulated in the triplet state will be $(n_i/4)k_{S'T} \times 10^{-6}$, where $k_{S'T}$ is the decay rate for non-radiative transitions from the first excited singlet state to the triplet state.

If we assume a 90% fluorescent quantum efficiency for the dye, neglect non-radiative transitions between first excited singlet and ground states, and assume again a 5-nsec fluorescence lifetime, we obtain a value for $k_{S'T}$ of about 2×10^7/sec. Then n_T works out to be $5n_i$—and the triplet-triplet loss is half the singlet-singlet gain. A border line lasing situation is thus implied under these conditions. Clearly, in order to avoid the necessity of a pumping flux much higher than the minimum theoretically required, *the risetime of the lamp should not exceed a few tenths of a microsecond.* The giant-pulse ruby laser rises in 10 nsec, and the clear advantage of this is now seen.

Our main conclusion here, therefore, is that a flashlamp capable of supplying light power on the order of 100 kW (in a band typically a few thousand cm^{-1} wide) and capable of reaching this maximum in a few tenths of a microsecond, should be an adequate source for powering a variety of organic dye lasers on a pulsed basis.

References

1. P. P. Sorokin & J. R. Lankard, *IBM Journal* 10, 162 (1966).
2. P. P. Sorokin, W. H. Culver, E. C. Hammond, and J. R. Lankard, *IBM Journal* 10, 401 (1966).
3. An account of this work is now available. See F. P. Schäfer, W. Schmidt, and J. Volze, *Appl. Phys. Lett.* 9, 306 (1966).
4. L. G. S. Brooker, "Absorption and Resonance in Dyes", *Rev. Mod. Phys.* 14, 275 (1942).
5. M. L. Spaeth and D. P. Bortfeld, *Appl. Phys. Lett.* 9, 179 (1966).
6. P. P. Sorokin, J. J. Luzzi, J. R. Lankard, and G. D. Pettit, *IBM Journal* 8, 182–184 (1964).
7. W. F. Kosonocky, S. E. Harrison, and R. Stander, *J. Chem. Phys.* 43m, 831 (1965).
8. F. Gires & F. Combaud, *Journ. de Physique* 26, 325 (1965); and F. Gires, *Quantum Electronics Conf.*, Phoenix, Ariz., April 1966.
9. M. L. Spaeth and W. R. Sooy, *Quantum Electronics Conf.*, Phoenix, Ariz., April 1966.
10. See for example, E. J. Bowen and D. Seaman, "The Efficiency of Solution Fluorescence", in *Luminescence of Organic and Inorganic Materials*, John Wiley & Sons, New York and London, 1962
11. D. Roess, "Giant Pulse Shortening by Resonator Transients", *J. Appl. Phys.* 37, 2004 (1966).
12. M. Goldstein, *Ordinary Differential Equations Solution by Runge-Kutta*, Share SDA 3240 (1964).
13. S. Gill, *Proc. Camb. Phil. Soc.* 47, 96 (1951).
14. O. D. Dmietrievskii, V. L. Ermolaev, and A. N. Terenin, *Doklady Akad. Nauk. SSSR* 114, 751 (1957).
15. G. P. Gurinovitch, A. N. Sevchenko, and K. N. Solov'ev, *Soviet Phys. Usp.* 6, No. 1, 67 (1963).
16. H. Kuhn, "The Electron Gas Theory of the Color of Natural and Artificial Dyes: Applications and Extensions," in *Progress in the Chemistry of Organic Natural Products*, edited by L. Zechmeister, Springer-Verlag OHG, Vienna, 1959.
17. P. P. Feofilov, "The Physical Basis of Polarized Emission", translated from the Russian, Consultants Bureau, New York, 1961. (Chap. 6, Sec. 2).
18. V. Zanker and E. Miethke, *Z. für Physikalische Chemie Neu Folge* 12, 13 (1957).
19. V. Zanker & E. Miethke, *Z. für Naturforsch.* 12a, 385 (1957).

Received October 14, 1966

Addendum: We have now observed stimulated emission from a number of dye solutions at wavelengths literally spanning the visible portion of the electromagnetic spectrum. The dyes with which lasing action was achieved are given below.

Dye	*Solvent*	*Molar Concentration*	*Fluorescence Peak*	*Color of Beam*
Acridine Red	Ethyl alcohol	10^{-3}	5800Å	Orange
Rhodamine 6G	Ethyl alcohol	$(3 - 300)\ 10^{-5}$	5550Å	Green-to-Orange
Eosin	Ethyl alcohol	10^{-3}	5400Å	Yellow
Fluorescein [a]	Water	10^{-3}	5270Å	Green
Fluorescein [a]	Ethyl alcohol	10^{-3}	5270Å	Green
Acridone	Ethyl alcohol	$>10^{-3}$	4370Å	Blue (4385Å)

[a] Fluorescein di-anion (sodium fluorescein)

Excitation was provided by a 3470Å giant-pulse laser beam used in combination with a transverse pumping geometry. The 3470Å beam was generated (at 10 MW) as the second harmonic of a 100-MW ruby laser beam by passing the latter through